Development 126, 1457-1466 (1999)
Printed in Great Britain © The Company of Biologists Limited 1999
DEV 7710

Bar homeobox genes are latitudinal prepattern genes in the developing *Drosophila* notum whose expression is regulated by the concerted functions of *decapentaplegic* and *wingless*

Makoto Sato, Tetsuya Kojima, Tatsuo Michiue and Kaoru Saigo*

Department of Biophysics and Biochemistry, Graduate School of Science, University of Tokyo, 7-3-1 Hongo, Bunkyo-ku, Tokyo 113-0033, Japan
*Author for correspondence (e-mail: saigo@biochem.s.u-tokyo.ac.jp)

Accepted 19 January; published on WWW 3 March 1999

SUMMARY

In *Drosophila* notum, the expression of *achaete-scute* proneural genes and bristle formation have been shown to be regulated by putative prepattern genes expressed longitudinally. Here, we show that two homeobox genes at the *Bar* locus (*BarH1* and *BarH2*) may belong to a different class of prepattern genes expressed latitudinally, and suggest that the developing notum consists of checker-square-like subdomains, each governed by a different combination of prepattern genes. *BarH1* and *BarH2* are coexpressed in the anterior-most notal region and regulate the formation of microchaetae within the region of *BarH1*/*BarH2* expression through activating *achaete-scute*. Presutural macrochaetae formation also requires *Bar* homeobox gene activity. *Bar* homeobox gene expression is restricted dorsally and posteriorly by Decapentaplegic signaling, while the ventral limit of the expression domain of *Bar* homeobox genes is determined by *wingless* whose expression is under the control of Decapentaplegic signaling.

Key words: *Bar*, *achaete-scute*, *decapentaplegic*, *wingless*, *Drosophila*, Prepattern gene

INTRODUCTION

The *Drosophila* notum is a two-dimensional sheet of patterned sensory bristles, macrochaetae and microchaetae. Macrochaetae are distributed in a limited number of loci while many microchaetae are formed in evenly spaced rows in wide areas of the notum. These bristles are derivatives of sensory organ precursors (SOPs), singled out from epidermal cells that express the proneural genes, *achaete* and *scute* (collectively called *ac-sc*; Ghysen et al., 1993). Thus, understanding how *ac-sc* expression is spatially and temporally regulated is a fundamental question in bristle patterning in the notum. *ac-sc* encodes basic helix-loop-helix (bHLH) proteins, and is regulated by many enhancer elements that may serve as targets for site-specific combinations of products of prepattern genes (Gomez-Skarmeta et al., 1995).

Several transcription factors have been shown to be involved in the regulation of *ac-sc* expression in the notum. *iroquois (iro)* homeobox genes are expressed longitudinally in the lateral notum and positively regulate *ac-sc* (Gomez-Skarmeta et al., 1996; Leyns et al., 1996; Kehl et al., 1998). *pannier (pnr)* encodes a GATA1-related transcriptional factor and is expressed longitudinally in the medial notum (Ramain et al., 1993; Calleja et al., 1996). Positive regulation of *ac-sc* by *pnr* is blocked by binding of U-shaped, a zinc finger protein (Cubadda et al., 1997; Haenlin et al., 1997). It has been proposed that the developing notum is divided into several longitudinal subdomains by the expression of prepattern genes essential for proneural gene expression (Calleja et al., 1996). *hairy* (*h*) and *extramacrochaetae* (*emc*) encode HLH proteins that negatively regulate *ac-sc*. H directly represses *ac-sc* transcription (Ohsako et al., 1994; Van Doren et al., 1994) while Emc does so indirectly. Emc prevents Daughterless (Da) from forming a heterodimer with Ac or Sc. Ac-Da and Sc-Da may be essential for the auto- and cross-activation of *ac-sc* (Skeath and Carroll, 1991; Van Doren et al., 1991; Cubas and Modolell, 1992; Van Doren et al., 1992). The concerted actions of these negative factors and prepattern gene products may be essential for temporal and spatial regulation of *ac-sc* expression and bristle formation.

Morphogen gradients are essential for cell fate determination in many developmental contexts (Lecuit et al., 1996; Nellen et al., 1996; Zecca et al., 1996; Lecuit and Cohen, 1997; Neumann and Cohen, 1997). In developing notum, Wingless (Wg), a secreted protein of Wnt family (Cadigan and Nusse, 1997), is expressed in a narrow longitudinal stripe and is necessary for bristle formation in its expression domain. *wg* is required for the formation of presutural (PS) macrochaetae, situated several cell diameters from the *wg* domain (Phillips and Whittle, 1993). Decapentaplegic (Dpp), a BMP family member (Hogan, 1996), is expressed along the anterior-posterior compartment border (Basler and Struhl, 1994;

Kojima et al., 1994; Tabata and Kornberg, 1994). The formation of dorso-central (DC) macrochaetae has recently been shown to require the concerted action of Dpp and Wg (Tomoyasu et al., 1998).

The present work shows *BarH1* and *BarH2*, homeobox genes at the *Bar* locus (Kojima et al., 1991; Higashijima et al., 1992a), to belong to a new class of putative prepattern genes expressed latitudinally and suggests that the developing notum consists of checker-square-like subdomains, each governed by a different combination of longitudinal and latitudinal prepattern genes. *Bar* homeobox genes are expressed in the anterior-most region (prescutum) and positively regulates *ac-sc* expression. The area of prescutum *Bar* expression is delimited by Dpp and Wg signaling. In addition, our results indicates that the gradient of Dpp signaling activity determines the domain of *wg* expression.

MATERIALS AND METHODS

Fly strains

Flies were raised at 25˚C except for temperature sensitive mutants, which were raised at 16.5˚C and 29˚C (or 25˚C), as the permissive and non-permissive temperatures respectively. Bar^{P058} is an enhancer trap line at the *Bar* locus and was obtained from FlyView. Deletion mutants at the *Bar* locus, $Df(1)B^{263\text{-}20}$ and *Df(1)BH2*, and f^{SH} (a strong hypomorphic allele of *f*) have been described (Higashijima et al., 1992b). As *Df(1)BH2*, its transgenic derivative possessing a *Fimbrin* (*Fim*) gene fragment was used. This derivative shows improved viability and fertility without changing bristle phenotypes and *Bar* expression (unpublished data). B^{25B} is a *BarH2* deletion mutant obtained upon relocation of P058 (see Fig. 3). Fly lines with *hs-BarH1* or *hs-BarH2* have been described (Kojima et al., 1991, 1993). $neur^{A101}$, an enhancer trap line at the *neuralized* locus, was used to mark SOPs and their progeny (Huang et al., 1991). iro^{1} (a viable hypomorphic allele of *iro*) and iro^{rF209} (an enhancer trap line at the *iro* locus) have been described (Gomez-Skarmeta et al., 1996). Allelic combinations of pnr^{VX1}, pnr^{V1}, and pnr^{D1} were used as *pnr* mutants (Ramain et al., 1993). wg^{Sp} is a regulatory mutant of *wg* (Neumann and Cohen, 1996), while wg^{IL114} (wg^{ts}) is a temperature sensitive allele of *wg*, having defects in Wg secretion (Gonzalez et al., 1991). Sources for Hw^{49c}, wg^{17en40}, dpp^{d12}, dpp^{d14}, dpp^{P10638} and hh^{9K} (hh^{ts}) are described in FlyBase. Sources for Gal4 trap lines (pnr^{md237} and *ap-Gal4*) and flies with *UAS-dpp*, *UAS-CD2*, and *UAS-NZ* (*UAS-lacZ*) are also described in FlyBase. Flies with *hs-FLPase*, tkv^{a12} *FRT40A* (Nellen et al., 1996), $arm^{H8.6}$ *FRT101* (Neumann and Cohen, 1997), *2πM FRT40A*, *NM FRT101*, *y FRT18A* (Xu and Rubin, 1993), *arm-lacZ FRT40A* (Lecuit and Cohen, 1997), and $Df(1)B^{263\text{-}20}$*,y FRT18A* were used for FLP/FRT-mediated mosaic analysis. Flies with *UAS>CD2, y*$^{+}$*>*tkv^{Q253D}, *UAS>CD2, y*$^{+}$*>flu-*Δ*arm*, *C765-Gal4* (Nellen et al., 1996; Zecca et al., 1996), and *arm-Gal4* (FlyBase) were used for generating transgene-expressing clones.

Plasmid construction and germline transformation

pUAS-BarH1 and pUAS-BarH2 were made by inserting a 2.1 kb *BarH1* cDNA fragment of pBH1B (Kojima et al., 1991) and a 2.2 kb *BarH2* cDNA fragment of p1-12 (Higashijima et al., 1992a) into the *Not*I site of pUASV, respectively. pUASV is a derivative of pYC1.8 (Fridell and Searles, 1991) and includes the UAS sequence (Brand and Perrimon, 1993) along with a single *Not*I site (unpublished data). pBgaV is a *Gal4 /vermilion* transformation vector, in which *Gal4* expression is regulated by B4.5 (see Fig. 3; unpublished data). pBN-Gal4 was constructed by inserting S8 (see Fig. 3) into the *Not*I site of pBgaV so that S8 was situated just upstream of B4.5. In pB4.5-lacZ, *lacZ* is under the control of B4.5, while, in pS8-BH2, *BarH2* associated with its core promoter is under the control of S8 (unpublished data). *UAS>CD2, y*$^{+}$*>BarH1* was constructed by T. Chimura and K. S. (unpublished data). Germline transformation was performed by standard procedures.

Immunohistochemistry

Immunostaining was carried out as described by Hayashi et al. (1998). Mouse anti-Ac (1:1 dilution; Skeath and Carroll, 1991), mouse anti-Wg (1:100; Neumann and Cohen, 1997), and rabbit anti-Sc (1:1000; Vaessin et al., 1994) antibodies were obtained from S. B. Carroll, S. M. Cohen and Y. N. Jan, respectively. Rabbit anti-LacZ (anti-β-gal; cappel), mouse anti-LacZ (promega), rabbit anti-BarH1 and anti-BarH2 (Higashijima et al., 1992a), respectively, were used in 1:2000, 1:1000, 1:100 and 1:20 dilution in the case of DAB staining. Five times higher concentrations of antibodies were used for fluorescence staining. Mouse anti-HA antibody (BAbCO), which recognizes the Flu-epitope, mouse anti-CD2 antibody (OX-34; Cedarlane Laboratories Ltd.), and mouse anti-Myc antibody (Ab-1; Oncogene Science) were used in 1:100 dilution. Target-gene-specific expression of LacZ was examined using Bar^{P058} (*Bar-lacZ*), $neur^{A101}$ (*neur-lacZ*), iro^{rF209} (*iro-lacZ*), wg^{17en40} (*wg-lacZ*) or dpp^{P10638} (*dpp-lacZ*) backgrounds.

Clonal analysis

FLP/FRT-mediated mosaic analysis was carried out as described previously (Nellen et al., 1996; Neumann and Cohen, 1997). Late second to early third or first to early second instar larvae were heat shocked and dissected after 44-48 or 68-84 hours, respectively. To obtain larger clones of $arm^{H8.6}$, heat-shocked larvae (first to early second instar) were raised at 16.5˚C for 3 days and then shifted to 25˚C for 44-48 hours before fixation. *hs-FLPase* was induced by a heat shock at 37˚C for 60-90 minutes to generate mutant clones, or at 34˚C for 30-60 minutes to generate clones expressing transgenes.

RESULTS

Restricted expression of *Bar* homeobox genes along the anterior notal edge

The *Drosophila* notum is considered genetically divided into several longitudinal domains (Calleja et al., 1996). To further clarify relative locations of *iro*, *wg* and *pnr* expression areas, third-instar larval and pupal future notum were stained with various combinations of molecular markers (Fig. 1A-K) and the results are schematically shown in Fig. 1N-P. In larval and pupal future notum, *pnr-Gal4* was expressed medially and *iro-lacZ* laterally (Fig. 1A,D,E,G). At variance with a previous prediction (Calleja et al., 1996), *pnr-Gal4* and *iro-lacZ* domains were found to partially overlap each other (compare Fig. 1A,H (I) with D,K), and *wg-lacZ* (or Wg) expression was noted in the *pnr-iro* overlapping region and its immediate neighbors (Fig. 1C,E,F).

Bar homeobox genes may belong to a class of notal subdivision genes different from *iro*, *wg* and *pnr*. Staining for BarH1 indicated that *BarH1* is expressed latitudinally in the anterior-most region of future notum and postnotum (Figs 1A,B,G, 2A,B). BarH1 expression began at early to mid third instar. Anti-Ac antibody staining and *neur-lacZ* expression indicated PS macrochaetae to be situated in the vicinity of posterior-ventral corners of the anterior BarH1 expression domain (Fig. 1L,M). Bar^{P058} is an enhancer trap line at the *Bar* locus. Double-staining Bar^{P058} larval discs for LacZ and BarH1 or BarH2 showed that *Bar-lacZ*, *BarH1* and *BarH2* are coexpressed (Fig. 2E,F). In the following, *BarH1* and *BarH2*

are referred to as *Bar* collectively and the anterior portion of the prescutum or its precursor expressing *Bar* as *Bar* prescutum. *Bar* expression similar to that in wing discs was observed in haltere discs (data not shown).

Requirement of *Bar* for bristle formation in anterior notum

For clarification of possible roles of *Bar* in notal development, we first carried out FLP/FRT-mediated mosaic analysis (Xu

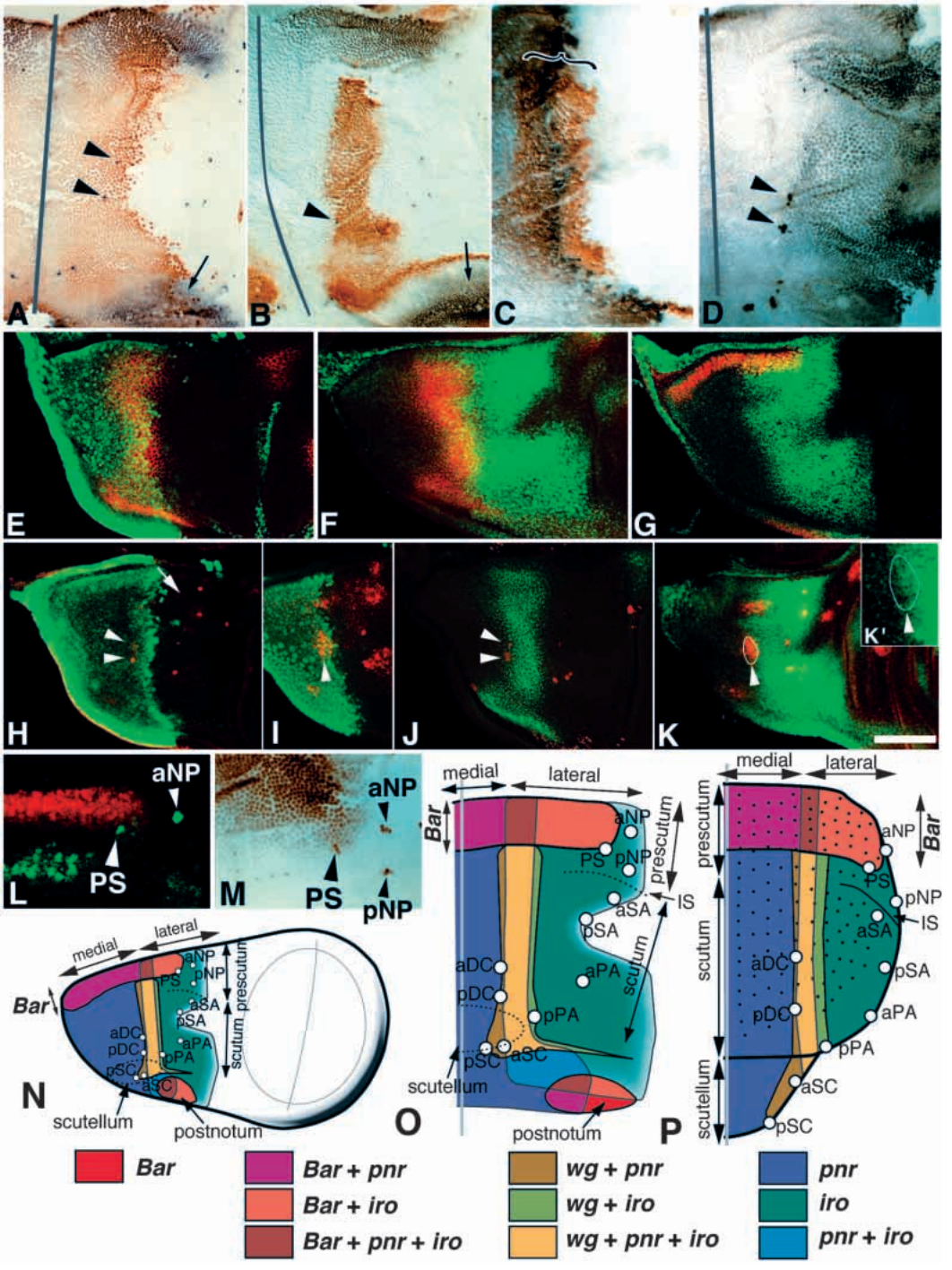

Fig. 1. Expression of putative prepattern genes in the developing notum at 8 hours APF (after puparium formation; A-D,M) and in late third-instar (E-L). Dorsal is left and anterior is up. Vertical bars, midlines. Macrochaetae cells were marked with BarH1 (A,B), *neur*-LacZ (D,J,M) or Ac (H,I,K,L). Arrowheads, dorso-central macrochaetae, aDC or pDC. Arrows in A and B, indicate postnotum BarH1 expression. (A) BarH1 (black); *UAS*-LacZ driven by *pnr-Gal4* (brown). Note that BarH1 is expressed in the anterior-most notum and postnotum. (B) BarH1 (black); *wg*-LacZ (brown). (C) *wg-lacZ*/+; *pnr-Gal4* /*UAS-CD2* flies were stained for CD2 (black) and LacZ (brown). The bracket shows that *wg*-LacZ expression partially overlaps *pnr-Gal4* expression. (D) *neur*-LacZ and *iro*-LacZ staining which were carried out simultaneously. *neur*-LacZ signals are much stronger than *iro*-LacZ signals. (E) Wg (red); *UAS*-LacZ driven by *pnr-Gal4* (green). (F) Wg (red); *iro*-LacZ (green). (G) BarH1(red); *iro*-LacZ (green). Note that *iro*-LacZ expression overlaps BarH1 expression in the anterolateral region. (H,I) Ac (red); *UAS*-LacZ driven by *pnr-Gal4* (green). The arrow in H indicates the PS macrochaetae cell position. Note the absence of clear Ac signals in this preparation. (J) *neur*-LacZ (red); Wg (green). (K) Ac (red); *iro*-LacZ (green). The DC macrochaetae proneural region is enclosed by a white line with an arrowhead. The discs in I,K are slightly younger than those in other panels. (K′) An enlargement of a part of K. Note that the DC proneural region is positive for both *iro*-LacZ (K,K′) and *pnr-Gal4* (I), indicating that *pnr-Gal4* and *iro*-LacZ domains partially overlap each other not only in pupae (see A-D) but also in larvae. (L,M) PS macrochaetae are situated near the posteroventral corner of the *Bar* prescutum at both larval (L) and pupal (M) stages. (L) BarH1 (red); Ac (green). (M) Simultaneous staining for *neur*-LacZ and BarH1. Isolated strong signals labeled PS, pNP and aNP correspond to *neur*-LacZ signals. (N-P) Schematic drawings of putative prepattern gene expression in the developing notum at late third instar larval (N) and early pupal (O) stages, and the extrapolated adult pattern (P). *Bar* is expressed latitudinally in the anterior edge, while *pnr*, *wg* and *iro* expression occur longitudinally. Small open circles show the position of 11 macrochaetae. IS, intrascutal suture. Scale bar (K) 50 μm for (A,B,D-K), 40 μm (C), 20 μm (L), and 30 μm (M).

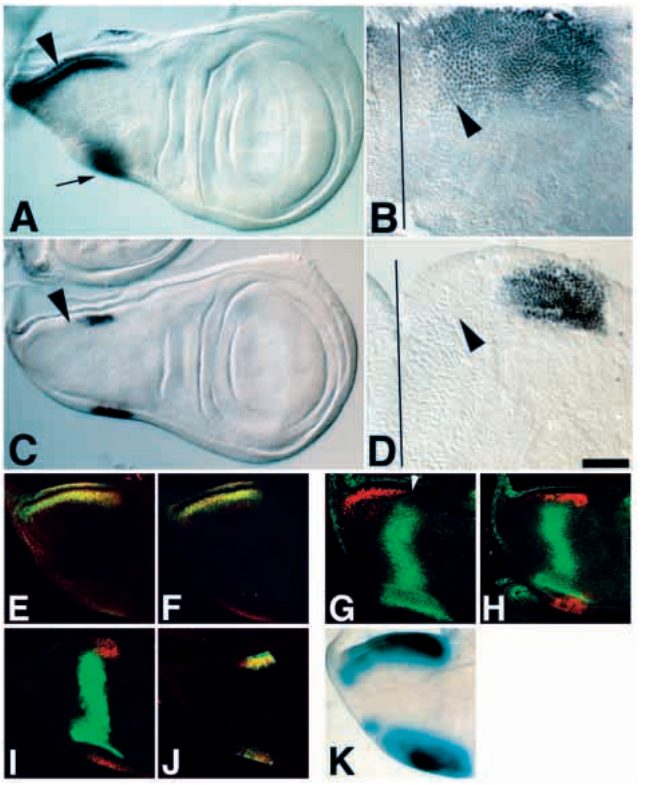

Fig. 2. Regulation of notal *Bar* by two enhancers. Dorsal (medial) is left, and anterior is up. (A,C,E-K) Late third-instar larval wing discs. (B,D) A part of the notum at 8 hours APF is shown. Vertical lines, midlines. (A-D) BarH1 expression in wild type (A,B) and in *Df(1)BH2* (C,D). Arrowheads in A and B indicate BarH1 expression in the prescutum, while those in C and D indicate the absence of BarH1 expression in the medial prescutum. Arrow, BarH1 expression in the future postnotum (a part of the peripordial membrane). (E) BarH1 (red); *Bar*-LacZ (green). That only yellow cells can be seen indicates the coexpression of BarH1 and *Bar*-LacZ in the anterior-most notal region. (F) BarH2 (red); *Bar*-LacZ (green). E and F together indicate that *BarH1* and *BarH2* are coexpressed in the notum. (G) BarH2 (red) driven by S8 in a *Df(1)BH2* background. Wg (green). As shown by the arrowhead, BarH2 expression is restricted to the dorsal *Bar* prescutum (arrowhead), suggesting that S8 is a medial prescutum *Bar* enhancer. (H) A wild type disc. B4.5-LacZ(red); Wg (green). (I) A *Df(1)BH2* disc. BarH1(red); *wg*-LacZ (green). (J) Coexpression of BarH1 (red) and B4.5-LacZ (green) in *Df(1)BH2*. H-J indicate that B4.5 is a lateral prescutum *Bar* enhancer. However, it should be noted that B4.5-LacZ expression in *Df(1)BH2* is restricted more ventrally than that in a wild-type background (compare H with J). (K) X-gal staining of *BN-Gal4*/*UAS-lacZ* nota. LacZ expression mimics wild-type BarH1 expression (see A). Scale bar in D, 50 μm (A,C,E-K), 30 μm (B,D).

and Rubin, 1993) using the *Df(1)B*$^{263\text{-}20}$ chromosome which uncovers *BarH1* and *BarH2* along with *forked* (*f*), *Fimbrin* (*Fim*), a broken *297* retrotransposon and an unknown gene *X2* (Fig. 3; Higashijima et al., 1992b; S. Ishimaru, T. K. and K. S., unpublished data). In this system, mutant cells are marked by *f*. Few microchaetae were generated in *Df(1)B*$^{263\text{-}20}$ clones within the prescutum (Fig. 4B). PS macrochaetae formation took place only when PS macrochaetae formation sites were not included within *Df(1)B*$^{263\text{-}20}$ clones. *Df(1)BH2* is a deletion at the *Bar* locus, uncovering *f*, *Fim* and *BarH2* (Fig. 3; Higashijima et al., 1992b). In flies hemizygous or homozygous for *Df(1)BH2*, the expression of *BarH1* in the medial *Bar* prescutum was totally absent (compare Fig. 2C,D with Fig. 2A,B), implying that *Df(1)BH2* uncovers a *Bar* enhancer specific to the medial *Bar* prescutum. In *Df(1)BH2* flies, microchaetae were lost medially in the anterior three quarters of the prescutum (Fig. 4C). PS macrochaetae were lost 60% of the time. Loss of *BarH1* expression and the microchaetae-less phenotype in the medial *Bar* prescutum were also detected in *Bar*^{25B} (Fig. 4D and data not shown), uncovering only *BarH2* and its 3′ *Bar* enhancer sequences (Fig. 3; see below). In *Bar*^{25B}, there was no PS macrochaetae formation (Fig. 4D). Taken together, these results suggest that *Bar* homeobox genes are essential for bristle formation in the *Bar* prescutum.

Should *Bar* homeobox genes be redundant in function and involved in bristle formation in the *Bar* prescutum, bristle defects would certainly be rescued by their targeted expression. These considerations were confirmed through the use of the GAL4/UAS system (Brand and Perrimon, 1993) along with *B*^{s}Y in a *Df(1)BH2* background. *UAS-BarH1* or *UAS-BarH2* was driven by *BN-Gal4*, a *Gal4* driver capable of mimicking wild-type *Bar* expression (see below). Loss of microchaetae but not PS macrochaetae was virtually restored by the targeted expression of *Bar* homeobox genes (Fig. 4E,F). PS macrochaetae loss in *Df(1)BH2* was rescued 100% of the time (*n*=30) by *B*^{s}Y containing *BarH1* but lacking the S8 *Bar* enhancer (see below) without rescuing microchaetae defects (Figs 3 and 4I). *BarH1* and *BarH2* would thus appear functionally redundant to each other and essential for microchaetae formation in the medial *Bar* prescutum and PS macrochaetae formation.

Identification of medial and lateral *Bar* enhancers

While searching for *Bar* enhancers, two notum enhancers were identified (T. M., unpublished data). S8, absent from *Df(1)BH2* and *B*^{25B} (Fig. 3), was found responsible for *Bar* expression in the medial *Bar* prescutum (Fig. 2G). B4.5 was

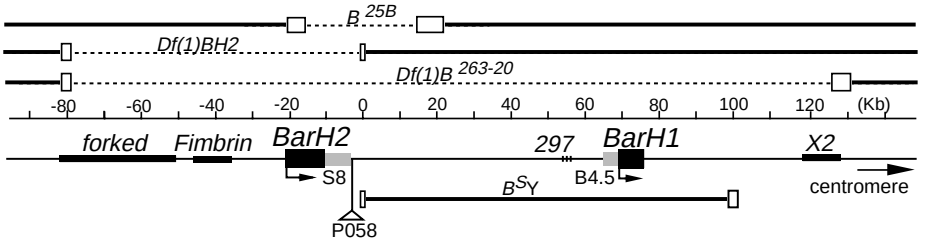

Fig. 3. Physical map of the *Bar* locus. Sizes and locations of *BarH1*, *BarH2*, *f*, *Fim*, and *X2* transcription units are indicated by filled boxes or bars, while *297* is indicated by three vertical bars. Stippled boxes labeled S8 and B4.5, respectively, show *Bar* enhancer specific for medial and lateral *Bar* prescutum expression. Sizes and locations of *Bar* deletions are shown above the scale, while the region covered by the *B*^{S}Y chromosome is given under the scale. Open boxes, ambiguities. Triangle, P058 insertion site.

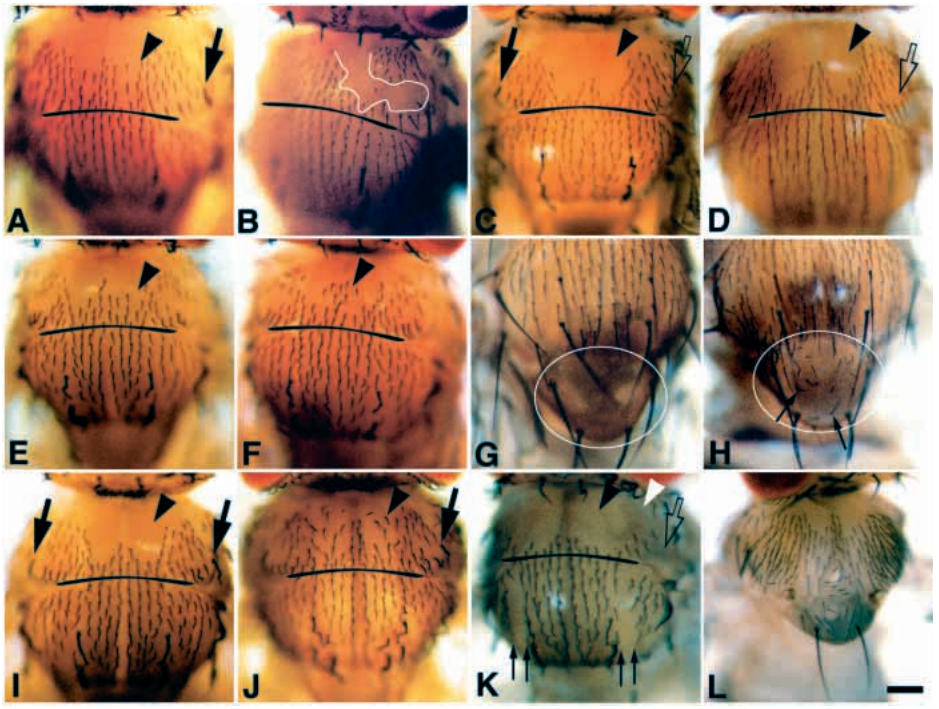

Fig. 4. Effects of *Bar* activity on notal bristle formation. Anterior is up. Black arrowheads show the presence or absence of microchaetae in the medial prescutum. Black horizontal lines drawn along IS indicate possible boundary between the prescutum and scutum. Thick filled and open arrows, respectively, show the presence and absence of PS macrochaetae. (A) Control (f^{SH} mutants). Except for the *f* phenotype, microchaetae are normally formed in the prescutum. (B) The absence of microchaetae from *Df(1)B*$^{263\text{-}20}$ mosaic clones in the prescutum. Note that there are only a few microchaetae in the mutant clone surrounded by a white line. Mutant clones were generated in first to early second instar larvae. (C,D) The absence of microchaetae from the medial prescutum of *Df(1)BH2* (C) and B^{25B} (D). The microchaetae-less phenotype of *Df(1)BH2* was rescued by *BN-Gal4*-driven *UAS-BarH1* (E) or *UAS-BarH2* (F). (G,H) Ectopic microchaetae formation in the scutellum due to heat-induction of *hs-BarH1*. The scutellum is enclosed by a white circle. (G) No heat induction (control). (H) A 20 minute, 36˚C heat induction at 6 hours APF. Thin arrows show ectopic microchaetae, most of which are out of focus. (I) *Df(1)BH2* defects in PS macrochaetae formation but not microchaetae formation were eliminated by $B^{s}Y$. (J) Suppression of the bristle-less phenotype of *Df(1)BH2* by Hw^{49c}. (K) The absence of medial (black arrowhead) and lateral (white arrowhead) microchaetae from *Df(1)BH2*; wg^{ts}/wg^{Sp} flies raised at 25˚C. Thin vertical arrows indicate the absence of microchaetae from the *wg* domain. This phenotype is not due to *Bar* activity. (L) Loss of scutum macrochaetae and notal size reduction by ubiquitous *BarH1* expression. *BarH1* was misexpressed throughout the notum by driving *UAS-BarH1* by *ap-GAL4*. All macrochaetae characteristic of the scutum (aSA, pSA, aPA, pPA, aDC and pDC) were lost. In addition, scutellum and prescutum macrochaetae were variably lost; aSC (90%, *n*=28), pSC (20%, *n*=28), PS (46%, *n*=28), pNP (96%, *n*=28) and aNP (0%, *n*=28). As with *hs-BarH1* induction, ectopic microchaetae formation occurred in the scutellum. Scale bar in (L) 100 μm.

capable of driving reporter gene (*lacZ*) expression in the lateral *Bar* prescutum in wild-type and *Df(1)BH2* backgrounds (Fig. 2H-J), although *lacZ* expression in the latter was restricted more ventrally than in the former. The *Bar* enhancer included in *BN-Gal4* is a composite of S8 and B4.5 so that expression of *UAS-lacZ* driven by *BN-Gal4* is capable of mimicking the endogeneous *Bar* expression (compare Fig. 2K and A).

Extra microchaetae formation by *Bar* misexpression at early pupal stages

To assess the capability of *Bar* for inducing microchaetae formation, *hs-BarH1* or *hs-BarH2* transgenes (Kojima et al., 1991, 1993) were heat-induced during larval or pupal development and the same results were obtained for each. Ectopic microchaetae were generated in the scutellum, wing blades and head capsule (Fig. 4H; data not shown). In the scutellum, normally possessing no microchaetae (Fig. 4G), 30-50 ectopic microchaetae were generated by a 36˚C 10 minute heat-shock at 6 hours APF (after puparium formation), but few ectopic microchaetae were formed by heat shock before 2 hours APF or after 12 hours APF. In contrast to ectopic microchaetae formation in neurogenic mutations (Ghysen et al., 1993), extra microchaetae induced by *hs-Bar* were unclustered (Fig. 4H), suggesting that *Bar* acts as an activator of proneural genes.

Bar as an *ac-sc* activator

Staining for Ac showed that pupal notum-specific Ac expression begins in characteristic regions at 6 hours APF, peaking at 8 hours APF and eventually disappearing at 12 hours APF (Fig. 5D). These Ac-positive regions appeared to correspond to microchaetae proneural regions since microchaetae SOP formation starts at 8 hours APF (Usui and Kimura, 1993). Macrochaetae SOP are formed during third instar (Huang et al., 1991). In the *Bar* prescutum, the area of Ac expression was seen to overlap that of *Bar* (Fig. 5A). Sc expression was quite similar, if not identical, to Ac expression (data not shown).

Study was thus made to find whether *Bar* is capable of acting as an activator of *ac-sc* to control microchaetae formation. Ac expression was almost entirely absent from the *Df(1)BH2* medial *Bar* prescutum (compare Fig. 5B and C), where no microchaetae formation took place (Fig. 4C). Following induction of *hs-Bar*, not only ectopic microchaetae formation (Fig. 4H) but strong Ac (and Sc) expression was apparent in the scutellum (compare Fig. 5D and E). *hs-Bar* dependent microchaetae formation was significantly suppressed in *ac-sc* hypomorphic mutant backgrounds (data not shown) while bristle defects including PS macrochaetae loss in *Df(1)BH2* were eliminated by Hw^{49c}, a gain-of-function allele of *ac-sc* (Fig. 4J). *Bar* may thus be considered to be an activator of *ac-sc* essential for producing proneural clusters for microchaetae and possibly PS macrochaetae as well.

Owing to weak transient Ac expression in the putative proneural region for PS macrochaetae, loss of the PS proneural region of Ac expression in a *Bar* mutant background could not be clearly demonstrated by antibody staining.

Regulation of *Bar* expression by Dpp and Wg signaling

During late third instar, the expression domain of *Bar* in the prescutum is immediately adjacent to *dpp* and *wg* expression domains (Figs 6A, 7A). *dpp* likely regulates *Bar* expression negatively. When *dpp* was expressed throughout the notum using *UAS-dpp* driven by *ap-Gal4*, *Bar* expression was totally abolished (Fig. 6E). Conversely, reduction in *dpp* activity ectopically induced *Bar* expression in the medial region of future notum (Fig. 6B). Similar medial expansion of *Bar* expression was observed subsequent to reduction in the activity of *hedgehog* (*hh*), an inducer of *dpp* (Fig. 6C; Basler and Struhl, 1994; Kojima et al., 1994; Tabata and Kornberg, 1994).

To more fully confirm the negative regulation of *Bar* expression by Dpp signaling, FLP/FRT-mediated mosaic analysis (Xu and Rubin, 1993; Nellen et al., 1996) was carried out. Clones in which Dpp signaling is constitutively active were generated using tkv^{Q253D}, which encodes a constitutively active form of a type I receptor of Dpp (Nellen et al., 1996). *Bar* expression was completely abolished irrespective of clone position (Fig. 6F,G). Cells in the *Bar* prescutum would thus appear to receive Dpp signals at the intensity less than the threshold level for *Bar* repression. Clones homozygous for tkv^{a12} (a strong hypomorphic allele of *tkv*) generated on the dorsal (medial) side of the notum were always associated with ectopic *Bar* expression (Fig. 6H,I). However, it should be noted that, in a large dorsal clone, *Bar* misexpression was restricted to its dorsal side (Fig. 6I). In clones generated near the posterior-dorsal edge of the endogenous *Bar* expression domain, *Bar* misexpression was restricted to a narrow region immediately adjacent to the endogeneous *Bar* domain (Fig. 6H). *Bar* misexpression was observed much less frequently in tkv^{a12} clones generated in or near the *wg* domain (Fig. 6K,L). In contrast, no appreciable change in *Bar* expression was detected in clones generated in the lateral notum (Fig. 6J).

Possible effects of *wg* on *Bar* expression was sought using wg^{ts}, in which Wg secretion but not production is temperature-sensitive (Gonzalez et al., 1991). *Bar* expression in the lateral *Bar* prescutum was abolished after 48 hours, but not 24 hours, incubation at 29˚C (Fig. 7C,D). Consistent with this, not only medial but also lateral microchaetae and PS macrochaetae were absent from *Df(1)BH2* flies transheterozygous for wg^{ts} and wg^{Sp}, raised at the non-permissive temperature (25˚C) (Fig. 4K). *armadillo* (*arm*), a β-catenin homologue, is a signal transducer of Wg signaling (Cadigan and Nusse, 1997). *Bar* expression was lost in clones mutant for *arm* when generated in the lateral *Bar* prescutum (Fig. 7E), while *Bar* misexpression was present in lateral prescutum clones expressing a constitutively active form of *arm* (*Δarm*; Fig. 7F). *Bar* expression in lateral prescutum is thus concluded to require Wg signals, whose levels determine the ventral border of the *Bar* prescutum.

During late third instar, the expression domain of *Bar* in the prescutum overlaps with those of *pnr* and *iro* (see Fig. 1E,G). Since no appreciable change in *Bar* expression was detected in flies mutant for *iro* or *pnr* (iro^1, pnr^{VX1}/pnr^{V1}, and pnr^{D1}/pnr^{V1}), *Bar* expression may be regulated independently of *pnr* and *iro*.

Negative regulation of *wg* expression by *Bar*

In wg^{17en40} flies mutant for *Df(1)BH2*, anterior expansion of *wg-lacZ* expression was found 50% of the time (Fig. 7B). Wg expression was repressed by *BarH1* misexpression (Fig. 7G,H). Thus, *Bar* may at least have partial involvement in the negative regulation of *wg*.

When *Bar* was expressed throughout the notum using *ap-*

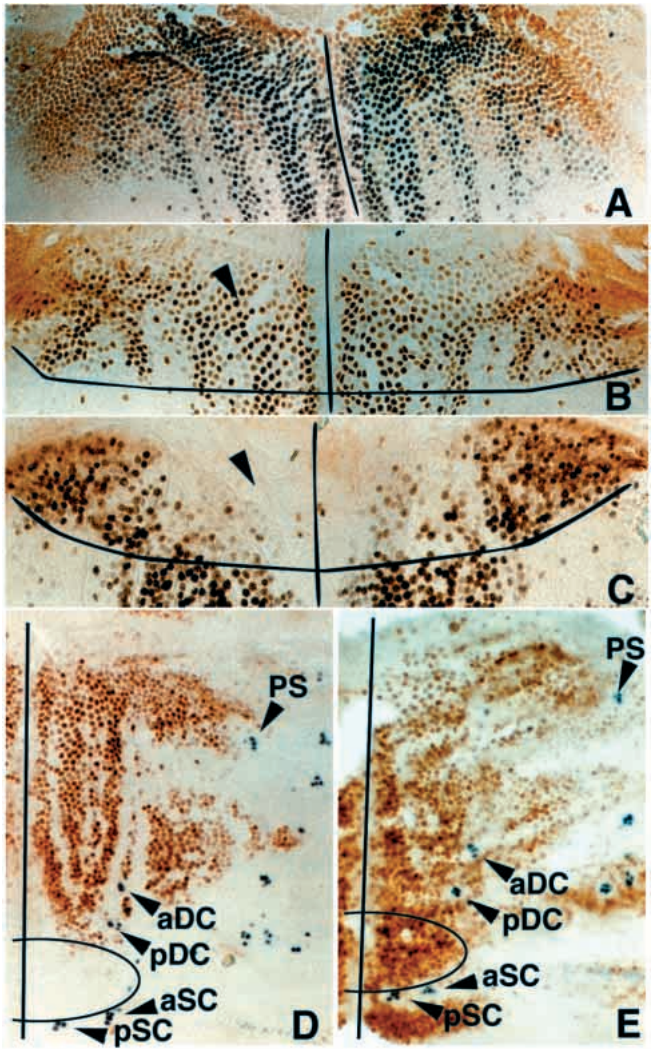

Fig. 5. Ac activation by *Bar* in the prescutum. Vertical lines, midline. (A) Ac expression overlaps *Bar* in the *Bar* prescutum. The notum at 8 hours APF was stained for *Bar*-LacZ (brown) and Ac (black). (B,C) Ac signals (nuclear signals black or brown) in *Df(1)BH2* (C) were significantly reduced in the medial *Bar* prescutum in comparison to wild type (B). B4.5-LacZ (non-nuclear brown signals) was used to mark the lateral prescutum (see Fig. 2H,I). Horizontal line, the posterior limit of the *Bar* prescutum inferred from B4.5-LacZ expression. (D) Ac expression of a wild type notum. Pupal nota were prepared at 8 hours APF, and stained for Ac (brown) and *neur*-LacZ (black; a marker for macrochaetae cells). (E) A *hs-BarH1* notum heat-shocked at 6 hours APF, and stained for Ac (brown) and *neur*-LacZ (black) at 8 hours APF. Half circles indicate scutella. Ac is strongly misexpressed in the scutellum. Scale bar in E 35 μm (A-C), 50 μm (D,E).

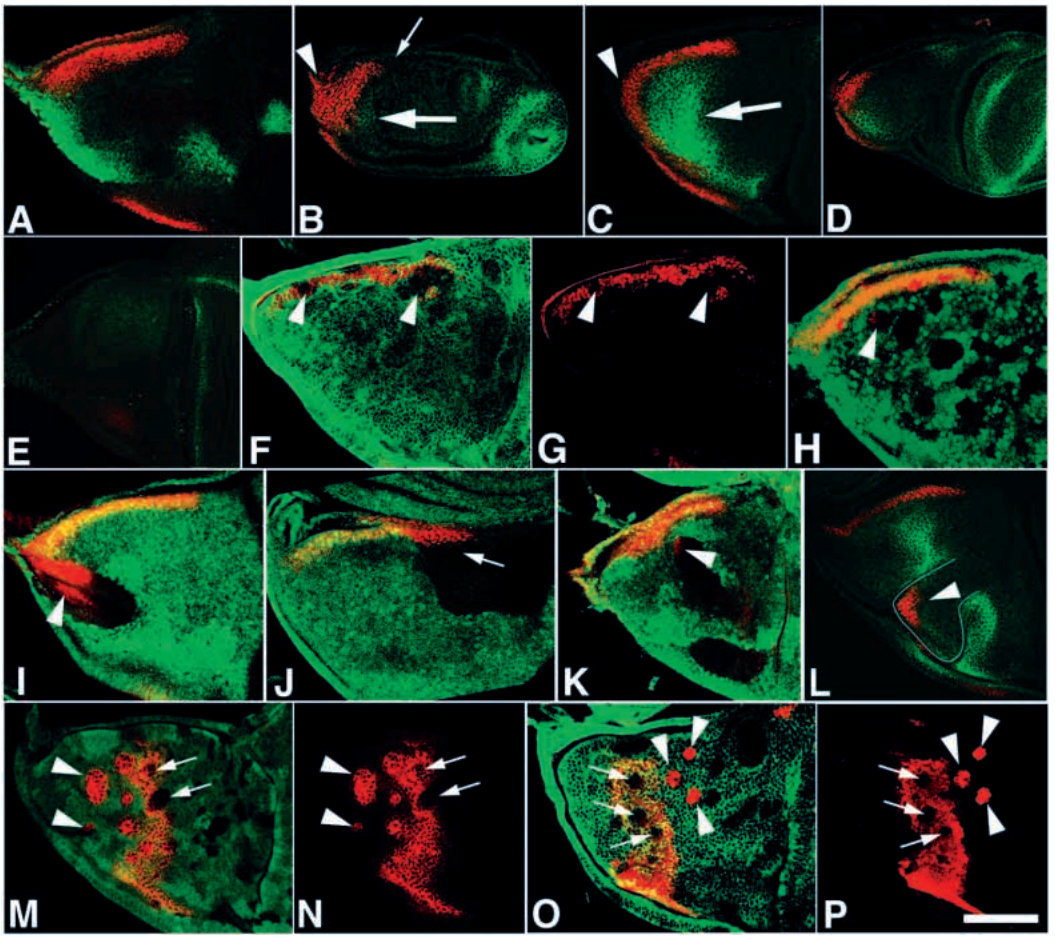

Fig. 6. Regulation of notal *Bar* and *wg* expression by Dpp signaling. The future nota of late third instar wing imaginal discs were examined. Anterior is up and dorsal is left. (A) Wild-type disc. BarH1 (red); *dpp*-LacZ (green). (B-E) BarH1 (red); Wg (green). (B) In a *dpp* strong disc mutant (dpp^{d12}/dpp^{d14}) background, the anterior *Bar* domain was expanded and shifted to the dorsal-most region of the notum (see arrowhead). Wg expression, which normally occurs in the central notum, was scarcely detectable in the vicinity of the dorsal Bar misexpression region (thick arrow). The thin arrow indicates the absence of *Bar* expression in the lateral prescutum. (C) In hh^{ts} discs treated at 29˚C for 48 hours before dissection, *Bar* and *wg* expression domains, respectively, shifted to the dorsal edge of the notum (arrowhead) and dorsally (thick arrow). (D) Prolonged *hh* inactivation (29˚C for 54 hours) resulted in further dorsal shift of *Bar* and *wg* expression domains; Wg signals were extensively reduced. (E) Both *BarH1* (red) and *wg* (green) were repressed in the future notum by *UAS-dpp* driven by *ap-Gal4*. (F,G) *BarH1* expression was abolished in all tkv^{Q253D} clones (arrowheads) generated in the *Bar* prescutum in late second to early third instar larvae. BarH1 (red); CD2 (green). The absence of CD2 shows the location of tkv^{Q253D} clones. tkv^{Q253D} was driven by *arm-Gal4*. (H-J) BarH1 (red); Myc (green). *BarH1* misexpression occurred in tkv^{a12} clones generated near the posterior border of the *Bar* prescutum (H; arrowhead) and in the dorsal side of the notum (I; arrowhead). No *BarH1* misexpression was detected in lateral notum clones (J; arrow). Mutant clones were generated in late second to early third instar (H), or in first to early second instar larvae (I,J). The absence of Myc shows the location of tkv^{a12} clones. Note that BarH1-positive clones in H and I, respectively, contain BarH1-negative cells in the posterior and ventral sides of the clones. (K,L) Less-frequent appearance of *BarH1* misexpression in tkv^{a12} clones generated in or near the central *wg* expression domain (see arrowheads in K,L) in first to second instar larvae. (K) BarH1 (red); Myc (green). (L) BarH1 (red); Wg (green). Note that the tkv^{a12} clone (outlined in L) lacks Wg expression. (M,N) Wg (red); *arm*-LacZ (green). The absence of *arm*-LacZ shows the location of tkv^{a12} clones. In tkv^{a12} clones within the *wg* domain, Wg expression was often abolished (see arrows). In mutant clones dorsal to the *wg* domain, Wg misexpression occurred (see arrowheads),while no Wg misexpression could be detected in clones lateral to the *wg* domain. (O,P) *wg*-LacZ (red); CD2 (green). In tkv^{Q253D} clones anterolateral to the *wg* domain, *wg*-LacZ was misexpressed (arrowheads), while *wg*-LacZ expression was abolished in clones within the *wg* domain (arrows). No Wg expression occurred in dorsal clones. Clones in M-P were generated in late second to early third instar larvae. Scale bar (P), 50 μm.

Gal4 and *UAS-Bar*, nearly all notal structures including pNP, aSA, pSA, aPA, pPA, aDC, pDC, and aSC macrochaetae were lost (Fig. 4L). Occasional loss of PS and pSC macrochaetae was also noted. Some of these phenotypes may be attributed to *wg* repression by *Bar*, since (1) the absence of *wg* results in loss of PS, aDC, pDC, pPA, aSC, pSC macrochaetae (Phillips and Whittle, 1993), and (2) notal *wg* expression was lost in *ap-Gal4*/*UAS-Bar* flies (Fig. 7G). Restriction of *Bar* expression to the anterior-most notum seems essential for normal subdivision of the notum.

Negative and positive regulation of notal *wg* expression by Dpp signaling

Fig. 6B,E indicates notal Wg expression to have been virtually completely abolished in strong disc mutants of *dpp* (dpp^{d12}/dpp^{d14}) and *UAS-dpp*/*ap-Gal4* flies expressing *dpp* throughout the notum. The *wg* expression domain shifted dorsally with reduction in the activity of Hh, a *dpp* inducer (Fig. 6C). The Hh activity of hh^{ts} flies was removed by a shift from 16.5 to 29˚C in mid-late second instar and a subsequent 48-hour incubation at 29˚C. Prolonged incubation at 29˚C not only enhanced dorsal shift of the *wg* domain but also caused considerable loss of Wg expression area (Fig. 6D). It thus follows that proper levels of Dpp signals may be essential for notal *wg* expression.

To determine whether there is an optimal range in Dpp signals for notal *wg* expression, examination was made of *wg* expression in loss-of-function (tkv^{a12}) and gain-of-function (tkv^{Q253D}) *tkv*

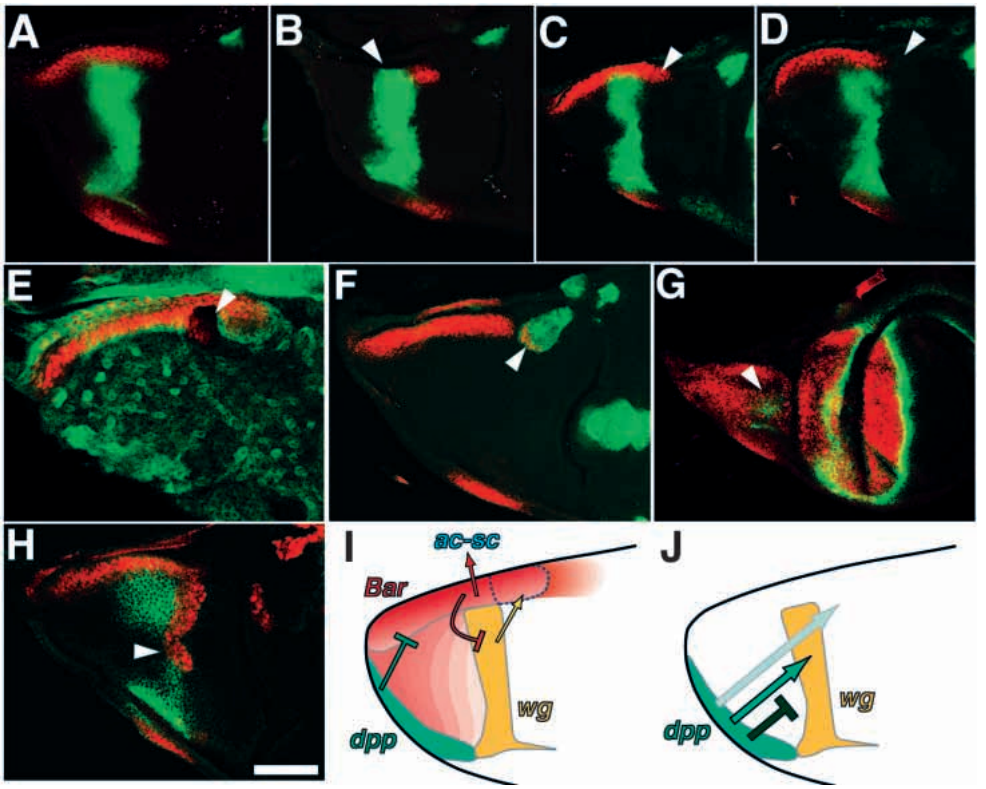

Fig. 7. Interactions between *Bar* and *wg* in the notum. Late third instar wing imaginal discs were examined. In all panels, BarH1 expression is shown by red. (A,B) *wg*-LacZ (green). (A) Wild type. The anterior BarH1 expression domain abuts on the central Wg expression domain. (B) *wg*-LacZ expression expanded anteriorly in *Df(1)BH2* (arrowhead) 50% of the time. (C,D) Wg (green). Bar expression in the lateral prescutum (see arrowheads) disappeared when wg^{ts} flies were raised at 29˚C for 48 hours (D), but not 24 hours (C), just before dissection. (E) Myc (green). $arm^{H8.6}$ clones are visualized by the absence of Myc. The arrowhead indicates the absence of *Bar* expression. (F) *BarH1* misexpression in Δ*arm* clones. Green, Flu-positive clones expressing the flu-tagged Δ*arm* driven by *C765-Gal4*. *BarH1* was misexpressed in a part of lateral prescutum clones (arrowhead). (G,H) notal Wg expression (green) was repressed by misexpression of *BarH1* throughout the notum (arrowheads, G; *ap-Gal4*/*UAS-BarH1*), or in clones ectopically expressing *BarH1* by *UAS-BarH1*/*ap-Gal4* (H). Clones were generated in first to early second (E,F), or in late second (H) instar larvae. (I) The regulation of *Bar* expression by *dpp* and *wg* is schematically shown. *Bar* expression is restricted dorsally and posteriorly by *dpp*, and activated by *wg* in the lateral prescutum. *wg* expression may be repressed by *Bar* in the anterior-most notum. *ac-sc* is positively regulated by *Bar*. (J) The regulation of *wg* expression by Dpp signaling is schematically shown. Notal *wg* expression requires optimal levels of Dpp signaling activity. Scale bar in H, 50 μm.

clones. tkv^{Q253D} was driven by *arm-Gal4*. In all cases, clones were generated during late second to early third instar and possible changes in *wg* expression were examined using anti-Wg or anti-LacZ antibodies in late third instar. *wg* misexpression was detected in all tkv^{a12} clones (n=17) dorsal to the authentic domain, while *wg* expression was absent from 30% of clones (n=24) generated within the authentic *wg* expression domain (Fig. 6M,N). No *wg* misexpression was present in ventral tkv^{a12} clones. The effects of tkv^{Q253D} differed from those of $tkv^{a12.}$ Two thirds of tkv^{Q253D} clones (n=66) anterolateral to the authentic *wg* domain were found to be associated with *wg* misexpression, while *wg* expression was abolished in 90% of clones (n=29) generated within the authentic *wg* expression domain (Fig. 6O,P). No *wg* expression was found in dorsal clones. An optimal range in Dpp signals may thus be concluded for notal *wg* expression (Fig. 7J) and it follows then that the notal *wg* domain can shift both dorsally and laterally depending on Dpp signaling intensity. In extreme cases, the *wg* domain may be totally eliminated from the notal region.

DISCUSSION

Bar homeobox genes as putative prepattern genes

We have shown that *BarH1* and *BarH2*, a pair of homeobox genes at the *Bar* locus, serve as putative prepattern genes for the anterior three quarters of the prescutum (*Bar* prescutum; see Fig. 1N-P). *BarH1* and *BarH2* are coexpressed in the *Bar* prescutum and required for transcriptional activation of proneural genes, *ac-sc*, and hence, bristle formation in the *Bar* prescutum. *BarH1* and *BarH2* appear functionally redundant to each other, since targeted expression of either *BarH1* or *BarH2* rescued microchaetae-less phenotypes of a *Bar*-deletion mutant (see Fig. 4E,F).

Bar genes may act as prepattern genes in tissues other than the notum. As with future notum, *Bar* is expressed in regions surrounding the compound eyes and regulates bristle formation (T. K., unpublished data). *Bar* misexpression brought about ectopic microchaetae formation in wing blades and the head capsule (unpublished data).

In embryonic external sensory organs, *Bar* is expressed in thecogen (glial cells) and neurons and is essential for sensillum subtype determination (Higashijima et al., 1992) *Bar* is also expressed in similar cells in nearly all adult sensory organs (T. K., unpublished data). However, in the progeny of SOPs, its expression was noted only in later stages of development and hence unrelated to region-specific *Bar* expression studied here.

Checker-board-like subdivisions of future notum by putative prepattern gene expression

Future notum may be divided into square subdomains in a checker-board-like manner, each with its own unique combinations of prepattern gene expression (see Fig. 1N-P). Putative prepattern genes, *iro* and *pnr*, form longitudinal domains. Here, we have shown *Bar* homeobox genes to form

the anterior-most latitudinal domain. To our knowledge, this is the first demonstration of the presence of latitudinal prepattern genes in the notum. Bristle formation in each subdomain may be positively regulated by a region-specific combination of prepattern genes. Consistent with this, our unpublished data disclose that microchaetae formation in the anterolateral prescutum (the lateral *Bar* prescutum), where *Bar* and *iro* are coexpressed (see Fig. 1G), requires the concerted action of *Bar* and *iro*.

Ac-Sc expression patterns differ in some respects with those of putative prepattern genes (compare Fig. 1O and Fig. 5D) and this would suggest the presence of a factor that restricts Ac-Sc expression spatially and/or temporally. Emc may possibly be such a factor, since notal Emc expression patterns at early pupal stages are partially complementary to those of Ac-Sc (unpublished data; see also Cubas and Modolell, 1992; Van Doren et al., 1992).

In various developmental contexts, determination of fate of a group of cells apparently depends on checker-board-like field subdivision along the anteroposterior and dorsoventral axes (Lawrence and Struhl, 1996). For example, the destiny of any given portion of the ectoderm, mesoderm and neuroectoderm in *Drosophila* may be determined by a combination of various genes expressed under the control of two-dimensional positional information provided by secretory and/or transcriptional factors (Azpiazu et al., 1996; Lawrence and Struhl, 1996; Skeath, 1998). Our study demonstrated that the two-dimensional sheet of *Drosophila* notum may be subdivided by a combination of longitudinal and latitudinal prepattern genes, suggesting that the checker-board-like subdivision of a developmental field may thus be a general developmental mechanism.

Regulation of *Bar* expression by Dpp and Wg signaling

Dpp and Wg have been shown to provide two-dimensional positional information in the wing pouch (Lecuit et al., 1996; Nellen et al., 1996; Zecca et al., 1996; Neumann and Cohen, 1997), but their roles in gene regulation in the notum should extend far beyond this. Our results (see Fig. 6A-E, M-P) show that the size and location of the notal *wg* expression domain vary depending on Dpp signaling activity. As schematically shown in Fig. 7J, strong Dpp signaling activity in the dorsal or medial region may repress *wg* expression while weak Dpp signals may determine the ventral limit of the authentic *wg* expression domain.

Clonal analysis (see Fig. 6F-L) indicated *Bar* expression in the prescutum to be negatively regulated by Dpp signaling (see Fig. 7I). Posterior and dorsal (medial) borders of the *Bar* prescutum domain is likely to be restricted directly by Dpp signals. *Bar* expression was always abolished in *tkv*-active (tkv^{Q253D}) clones no matter where situated in the *Bar* prescutum (Fig. 6F,G) while *Bar* misexpression was restricted to *tkv*-negative (tkv^{a12}) clones in the dorsal notum (Fig. 6H-L). Dpp signal activity in the ventral notum may thus perhaps be less than that required for *Bar* repression.

Lateral *Bar* expression in the prescutum is positively regulated by *wg* (see Fig. 7C-F). Ectopic *Bar* expression in *Δarm* clones generated in the lateral prescutum suggests that a narrow anterior region situated more ventral to the *Bar* prescutum is *wg*-susceptible and thus the ventral border of *Bar* expression domain in the prescutum may be determined by Wg signals (Fig. 7I). Loss of *Bar* expression from the lateral prescutum in *dpp* mutants (see thin arrow in Fig. 6B) may be a secondary effect arising from the loss of Wg expression in *dpp* mutants, since *Bar* expression was not abolished in *tkv*-negative clones in the lateral prescutum (see Fig. 6J).

Fig. 2H suggests that the lateral *Bar* enhancer for microchaetae formation may be included in fragment B4.5. Thus, a transcription factor situated downstream of Wg signaling might recognize and bind to sites in B4.5 so as to activate *Bar* and hence *ac-sc*. PS macrochaetae formation requires not only *Bar* but also *wg* (Phillips and Whittle, 1993) and accordingly a similar cascade including *wg*, *Bar* and *ac-sc* may be involved in PS macrochaetae formation. However, that PS macrochaetae defects in *Df(1)BH2* are rescued by B^S Y but not *UAS-Bar* driven by *BN-Gal4* may be indication that *cis*-regulatory elements essential for PS macrochaetae formation are included in B^S Y but neither in S8 nor B4.5.

We are grateful to K. Basler, A. Bejsovec, S. M. Cohen, J. L. Gomez-Skarmeta, S. Hayashi, J. Modolell, P. Simpson, G. Struhl, T. Tabata, R. Ueda, T. Uemura and the stock centers of Bloomington, and FlyView for fly strains, and to S. B. Carroll, S. M. Cohen and Y. N. Jan for antibodies. This work was supported in part by grants from the Ministry of Education, Science and Culture of Japan to K. S.

REFERENCES

Azpiazu, N., Lawrence, P. A., Vincent, J. P., and Frasch, M. (1996) Segmentation and specification of the *Drosophila* mesoderm. *Genes. Dev.* **10**, 3183-3194.

Basler, K. and Struhl, G. (1994). Compartment boundaries and the control of *Drosophila* limb pattern by *hedgehog* protein. *Nature* **368**, 208-214.

Brand, A. H. and Perrimon, N. (1993). Targeted gene expression as a means of altering cell fates and generating dominant phenotypes. *Development* **118**, 401-415.

Cadigan, K. M. and Nusse, R. (1997). Wnt signaling: A common theme in animal development. *Genes Dev.* **11**, 3286-3305.

Calleja, M., Moreno, E., Pelaz, S. and Morata, G. (1996). Visualization of gene expression in living adult *Drosophila*. *Science* **274**, 252-255.

Cubadda, Y., Heitzler, P., Ray, R. P., Bourouis, M., Ramain, P., Gelbart, W., Simpson, P. and Haenlin, M. (1997). *u-shaped* encodes a zinc finger protein that regulates the proneural genes *achaete* and *scute* during the formation of bristles in *Drosophila*. *Genes Dev.* **11**, 3083-3095.

Cubas, P. and Modolell, J. (1992). The *extramacrochaetae* gene provides information for sensory organ patterning. *EMBO J.* **11**, 3385-3393.

Fridell, Y. W. C. and Searles., L. L. (1991). *vermilion* as a marker gene for *Drosophila* transformation. *Nucleic Acids Res.* **19**, 5082.

Ghysen, A., Dambly-Chaudiere, C., Jan, L. Y. and Jan, Y. N. (1993). Cell interaction and gene interaction in peripheral neurogenesis. *Genes Dev.* **7**, 723-733.

Gomez-Skarmeta, J. L., del Corral, R. D., de la Calle-Mustienes, E., Ferre-Marco, D. and Modolell, J. (1996). *araucan* and *caupolican*, two members of the novel *iroquois* complex, encode homeoproteins that control proneural and vein-forming genes. *Cell* **85**, 95-105.

Gomez-Skarmeta, J. L., Rodriguez, I., Martinez, C., Culi, J., Ferres-Marco, D., Beamonte, D. and Modolell, J. (1995). *Cis*-regulation of *achaete* and *scute*: shared enhancer-like elements drive their coexpression in proneural clusters of the imaginal discs. *Genes Dev*. **9**, 1869-1882.

Gonzalez, F., Swales, L., Bejsovec, A., Skaer, H. and Martinez Arias, A. (1991). Secretion and movement of Wingless protein in the epidermis of the *Drosophila* embryo. *Mech. Dev.* **35**, 43-54.

Haenlin, M., Cubadda, Y., Blondeau, F., Heitzler, P., Lutz, Y., Simpson, P. and Ramain, P. (1997). Transcriptional activity of Pannier is regulated negatively by heterodimerization of the GATA DNA-binding domain with a cofactor encoded by the *u-shaped* gene of *Drosophila*. *Genes Dev.* **11**, 3096-3108.

Hayashi, T., Kojima, T. and Saigo, K. (1998). Specifiation of primary

pigment cell and outer photoreceptor fates by *BarH1* homeobox gene in the developing *Drosophila* eye. *Dev. Biol.* **200**, 131-145.

Higashijima, S., Kojima, T., Michiue, T., Ishimaru, S., Emori, Y. and Saigo, K. (1992a). Dual *Bar* homeo box genes of *Drosophila* required in two photoreceptor cells, R1 and R6, and primary pigment cells for normal eye development. *Genes Dev.* **6**, 50-60.

Higashijima, S., Michiue, T., Emori, Y. and Saigo, K. (1992b). Subtype determination of *Drosophila* embryonic external sensory organs by redundant homeo box genes *BarH1* and *BarH2*. *Genes Dev.* **6**, 1005-1018.

Hogan, B. L. (1996). Bone morphogenetic proteins: multifunctional regulators of vertebrate development. *Genes Dev.* **10**, 1580-1594.

Huang, F., Dambly-Chaudiere, C. and Ghysen, A. (1991). The emergence of sense organs in the wing disc of *Drosophila*. *Development* **111**, 1087-1095.

Kehl, B. T., Cho, K. and Choi, K. (1998). *mirror*, a *Drosophila* homeobox gene in the *iroquois* complex, is required for sensory organ and alula formation. *Development* **125**, 1217-1227.

Kojima, T., Ishimaru, S., Higashijima, S., Takayama, E., Akimaru, H., Sone, M., Emori, Y. and Saigo, K. (1991). Identification of a different-type homeobox gene, *BarH1*, possibly causing *Bar (B)* and *Om(1D)* mutations in *Drosophila*. *Proc. Natl. Acad. Sci. USA* **88**, 4343-4347.

Kojima, T., Michiue, T., Orihara, M. and Saigo, K. (1994). Induction of a mirror-image duplication of anterior wing structures by localized *hedgehog* expression in the anterior compartment of *Drosophila* melanogaster wing imaginal discs. *Gene* **148**, 211-217.

Kojima, T., Sone, M., Michiue, T. and Saigo, K. (1993). Mechanism of induction of *Bar*-like eye malformation by transient overexpression of *Bar* homeobox genes in *Drosophila* melanogaster. *Genetica* **88**, 85-91.

Lawrence, P. A. and Struhl, G. (1996). Morphogens, Compartments, and Pattern: Lessons from *Drosophila*? *Cell* **85**, 951-961.

Lecuit, T., Brook, W. J., Ng, M., Calleja, M., Sun, H. and Cohen, S. M. (1996). Two distinct mechanisms for long-range patterning by Decapentaplegic in the *Drosophila* wing. *Nature* **381**, 387-393.

Lecuit, T. and Cohen, S. M. (1997). Proximal-distal axis formation in the *Drosophila* leg. *Nature* **388**, 139-145.

Leyns, L., Gomez-Skarmeta, J. L. and Dambly-Chaudiere, C. (1996). *iroquois*: a prepattern gene that controls the formation of bristles on the thorax of *Drosophila*. *Mech. Dev.* **59**, 63-72.

Nellen, D., Burke, R., Struhl, G. and Basler, K. (1996). Direct and long-range action of a DPP morphogen gradient. *Cell* **85**, 357-368.

Neumann, C. J. and Cohen, S. M. (1996). *Sternopleural* is a regulatory mutation of *wingless* with both dominant and recessive effects on larval development of *Drosophila melanogaster*. *Genetics* **142**, 1147-1155.

Neumann, C. J. and Cohen, S. M. (1997). Long-range action of Wingless organizes the dorsal-ventral axis of the *Drosophila* wing. *Development* **124**, 871-880.

Ohsako, S., Hyer, J., Panganiban, G., Oliver, I. and Caudy, M. (1994). Hairy function as a DNA-binding helix-loop-helix repressor of *Drosophila* sensory organ formation. *Genes Dev*. **8**, 2743-2755.

Phillips, R. G. and Whittle, J. R. (1993). *wingless* expression mediates determination of peripheral nervous system elements in late stages of *Drosophila* wing disc development. *Development* **118**, 427-438.

Ramain, P., Heitzler, P., Haenlin, M. and Simpson, P. (1993). *pannier*, a negative regulator of *achaete* and *scute* in *Drosophila*, encodes a zinc finger protein with homology to the vertebrate transcription factor GATA-1. *Development* **119**, 1277-1291.

Skeath, J. B. and Carroll, S. B. (1991). Regulation of *achaete-scute* gene expression and sensory organ pattern formation in the *Drosophila* wing. *Genes Dev*. **5**, 984-995.

Skeath, J. B. (1998). The *Drosophila* EGF receptor controls the formation and specification of neuroblasts along the dorsal-ventral axis of the *Drosophila* embryo. *Development* **125**, 3301-3312.

Tabata, T. and Kornberg, T. B. (1994). Hedgehog is a signaling protein with a key role in patterning *Drosophila* imaginal discs. *Cell* **76**, 89-102.

Tomoyasu, Y., Nakamura, M. and Ueno, N. (1998). Role of Dpp signaling in pattern formation of the dorsocentral mechanosensory organ in *Drosophila* melanogaster. *Development* **125**, 4215-4224.

Usui, K. and Kimura, K. (1993). Sequential emergence of the evenly spaced microchaetes on the notum of *Drosophila*. *Roux's Arch. Dev. Biol.* **203**, 151-158.

Vaessin, H., Brand, M., Jan, L. Y. and Jan, Y. N. (1994). *daughterless* is essential for neuronal precursor differentiation but not for initiation of neuronal precursor formation in *Drosophila* embryo. *Development* **120**, 935-945.

Van Doren, M., Bailey, A. M., Esnayra, J., Ede, K. and Posakony, J. W. (1994). Negative regulation of proneural gene activity: hairy is a direct transcriptional repressor of *achaete*. *Genes Dev*. **8**, 2729-2742.

Van Doren, M., Ellis, H. M. and Posakony, J. W. (1991). The *Drosophila extramacrochaetae* protein antagonizes sequence-specific DNA binding by *daughterless/achaete-scute* protein complexes. *Development* **113**, 245-255.

Van Doren, M., Powell, P. A., Pasternak, D., Singson, A. and Posakony, J. W. (1992). Spatial regulation of proneural gene activity: auto- and cross-activation of *achaete* is antagonized by *extramacrochaetae*. *Genes Dev*. **6**, 2592-2605.

Xu, T. and Rubin, G. M. (1993). Analysis of genetic mosaics in developing and adult *Drosophila* tissues. *Development* **117**, 1223-1237.

Zecca, M., Basler, K. and Struhl, G. (1996). Direct and long-range action of a Wingless morphogen gradient. *Cell* **87**, 833-844.